Supporting Information For

Magnetoresistive Polyaniline/Multi-Walled Carbon Nanotubes Nanocomposites with Negative Permittivity

Hongbo Gu,[†,‡] Jiang Guo,[†,#] Qingliang He,[†,#] Yuan Jiang,[†] Yudong Huang,[‡] Zhiping Luo,[§] Neel Haldolaarachige,[∏] David P. Young,[∏] Suying Wei[†,#,*] and Zhanhu Guo[†*]

[†]Integrated Composites Lab (ICL), Dan F. Smith Department of Chemical Engineering, Lamar University, Beaumont, TX 77710 USA

[‡]School of Chemical Engineering and Technology, Harbin Institute of Technology, Harbin, Heilongjiang 150001 China

[#]Department of Chemistry and Biochemistry, Lamar University, Beaumont, TX 77710 USA

[§]Department of Chemistry and Physics, Fayetteville State University, Fayetteville, NC 28301 USA

[∏] Department of Physics and Astronomy, Louisiana State University, Baton Rouge, LA 70803 USA

*Corresponding author

E-mail: suying.wei@lamar.edu (S.W.) and zhanhu.guo@lamar.edu (Z.G.)

S1. Experimental

S1.1 Materials

MWNTs (SW*e*NT SMW 200X, average diameter: 10.4 nm; average length: 4.3 μm) were provided by SouthWest NanoTechnologies. Aniline (C_6H_7N), ammonium persulfate (APS, $(NH_4)_2S_2O_8$) and *p*-toluene sulfonic acid (PTSA, $C_7H_8O_3S$) were purchased from Sigma Aldrich. Potassium dichromate ($K_2Cr_2O_7$) was purchased from Alfa Aesar Company. Methanol was obtained from Fisher Scientific. All the chemicals were used as-received without any further treatment.

S1.2 Synthesis of MWNTs/PANI PNCs

The MWNTs/PANI PNCs were fabricated with the SIP method. The potassium dichromate ($K_2Cr_2O_7$) stock solution was prepared by dissolving potassium dichromate (1.1315 g) in deionized water (100.0 mL) to give a concentration of 4.0 g L^{-1}. The Cr(VI) solution was prepared by diluting $K_2Cr_2O_7$ stock solution with deionized water and the mixed ratio of Cr(VI) and PTSA was 1: 10. First, PTSA (15.0 mmol) was added into 100.0 mL Cr(VI) solution with an adjusted pH of 1.0 aiming to introduce surface functional groups.[1] Then the MWNTs were dispersed in the above solution in an ice-water bath for one-hour sonication combined with mechanical stirring. After that, the aniline solution (18.0 mmol in 25.0 mL deionized water, molar ratio of Cr(VI): PTSA: aniline = 1 : 10 : 12) was mixed with the above MWNTs suspension, which was mechanically and ultrasonically stirred continuously for additional two hours in an ice-water bath for further polymerization. The product was vacuum filtered and washed with deionized water. The precipitant was further washed with methanol to remove any possible oligomers. The final MWNTs/PANI PNCs were dried at 50 ^{o}C in an oven

overnight. The PNCs with a MWNT loading of 5.0, 10.0 and 20.0 wt% were fabricated (the products were named as T5, T10, T20, respectively). Pure PANI was also fabricated following the above same procedures without adding any MWNTs for comparison with T5, T10 and T20 samples.

The aniline was further polymerized on T20 by APS (the loading of T20 in the final PNCs was controlled at 5.0 wt%) and the product was named as T205. Briefly, the T20 (0.0881 g) was dispersed in 100.0 mL deionized water in an ice-water bath for one-hour sonication combined with mechanical stirring. Then the aniline solution (18.0 mmol in 25.0 mL deionized water with the molar ratio of APS: PTSA: aniline = 3: 5: 6) was added into the above mixed solution and mechanically and ultrasonically stirred continuously for additional two hours in an ice-water bath for further polymerization. After that, the sample was vaccum filtered and washed with deionized water and methanol. The final sample was dried at 50 ^{o}C in an oven overnight. Meanwhile, the aniline was further polymerized on T20 by $K_2Cr_2O_7$ (3.0 mmol) with a molar ratio of $K_2Cr_2O_7$: PTSA: aniline = 1: 5: 6 following the above procedures and the loading of T20 for the final PNCs was 5.0 wt% (the product was named as TCr205). The PNCs containing 5.0 wt% as-received MWNTs were also prepared by oxidizing aniline by APS with a molar ratio of APS: PTSA: aniline = 3: 5: 6 following the above procedures (the product was named as TA05). These three samples (T205, TCr205 and TA05) were prepared for comparison with the T5 sample.

S1.3 Characterizations

The chemical structure of the synthesized PNCs was tested by the Fourier transform infrared spectroscopy (FT-IR, a Bruker Inc. Vector 22 coupled with an ATR

accessory) in the range of 500 to 2500 cm^{-1} at a resolution of 4 cm^{-1}. The thermal stability of the synthesized PNCs was conducted in a thermogravimetric analysis (TGA, TA instruments, Q-500) with a heating rate of 10 ^{o}C min^{-1} under an air flow rate of 60 mL min^{-1} from 25 to 800 ^{o}C.

The morphologies of the as-received MWNTs and the synthesized PNCs were observed on a JEOL JSM-6510LV scanning electron microscopy (SEM) after coated with carbon. The as-received MWNTs and the synthesized PNCs were further characterized by a transmission electron microscopy (TEM, FEI Tecnai G2 F20) with a field emission gun, operated at an accelerating voltage of 200 kV. The TEM samples were prepared by drying a drop of samples/ethanol suspension on carbon-coated copper TEM grids.

Raman spectra were obtained using a Horiba Jobin-Yvon LabRam Raman Confocal Microscope with 785 and 633nm laser excitations at a 1.5 cm^{-1} resolution at room temperature. The X-ray photoelectron spectroscopy (XPS) measurements were performed in a Kratos AXIS 165 XPS/AES instrument using monochromatic Al Kα radiation. The Cr2p peaks were deconvoluted into the components consisting of a Gaussian line shape Lorentzian function (Gaussian = 80 %, Lorentzian= 20 %) on Shirley background.

Dielectric properties were investigated by a LCR meter (Agilent, E4980A) equipped with a dielectric test fixture (Agilent, 16451B) at the frequency of 20 to 2×10^{6} Hz at room temperature. The as-received MWNTs, pure PANI and their PNC powders were pressed in a form of disc pellet with a diameter of 25 mm by applying a pressure of 50 MPa in a hydraulic presser and the average thickness was about 1.0 mm. The same sample for LCR measurement was also used to measure the resistivity (ρ) by a standard

four-probe method from 50 to 290 K. The temperature dependent resistivity was used to determine the electrical conduction mechanism in the as-received MWNTs, pure PANI and their PNCs. Magnetoresistance was carried out using a standard four-probe technique by a 9-Tesla Physical Properties Measurement System (PPMS) by Quantum Design at room temperature. The four probes were 0.002 inch diameter platinum wires, which were attached by silver paste to the sample. And the magnetic field was applied perpendicular to the current.

S2. Morphology of MWNTs/PANI PNCs

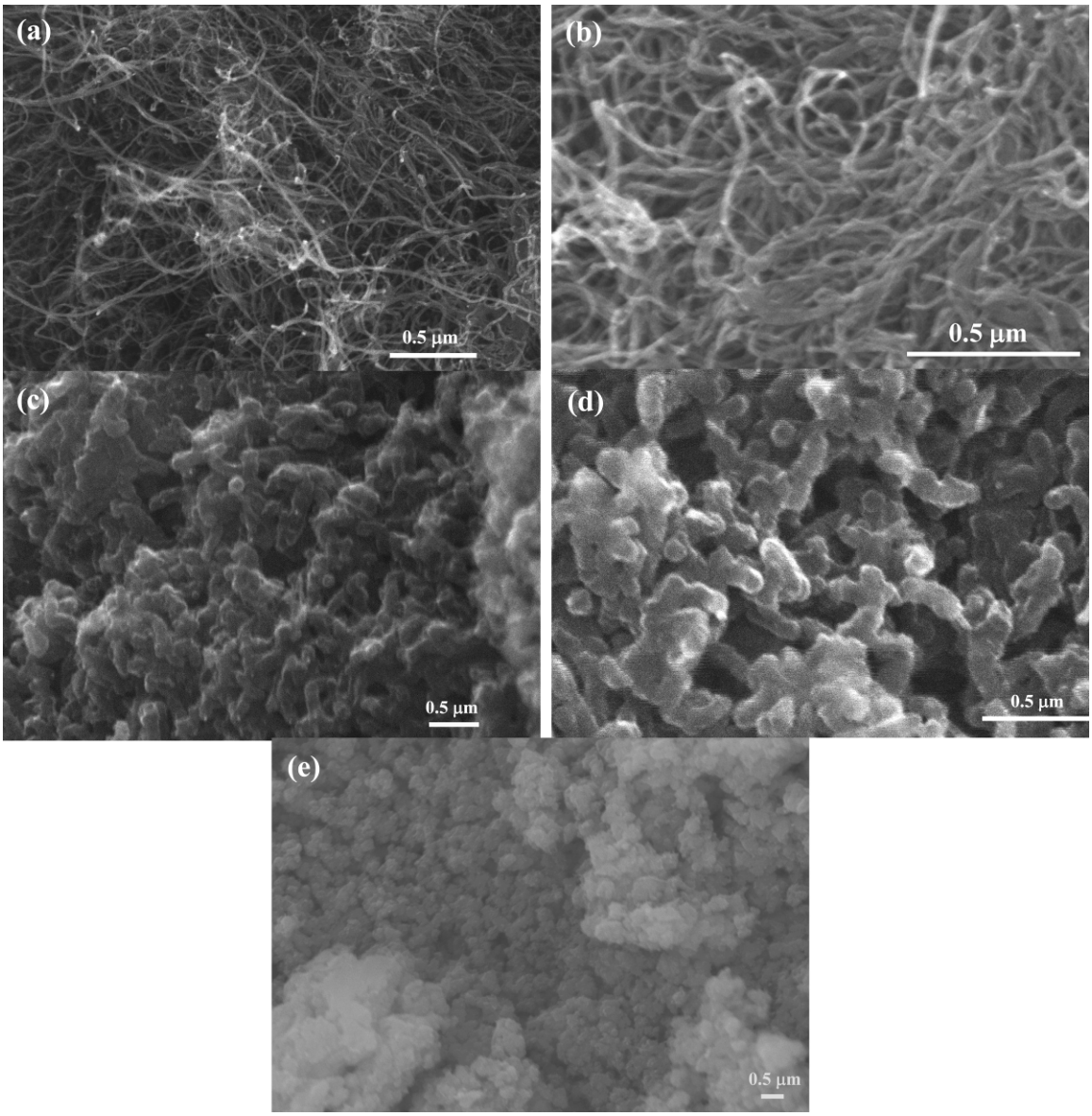

Fig. S1 SEM images of the (a) as-received MWNTs, (b) T20, (c) T205, (d) TCr205, and (e) PANI oxidized by Cr(VI).

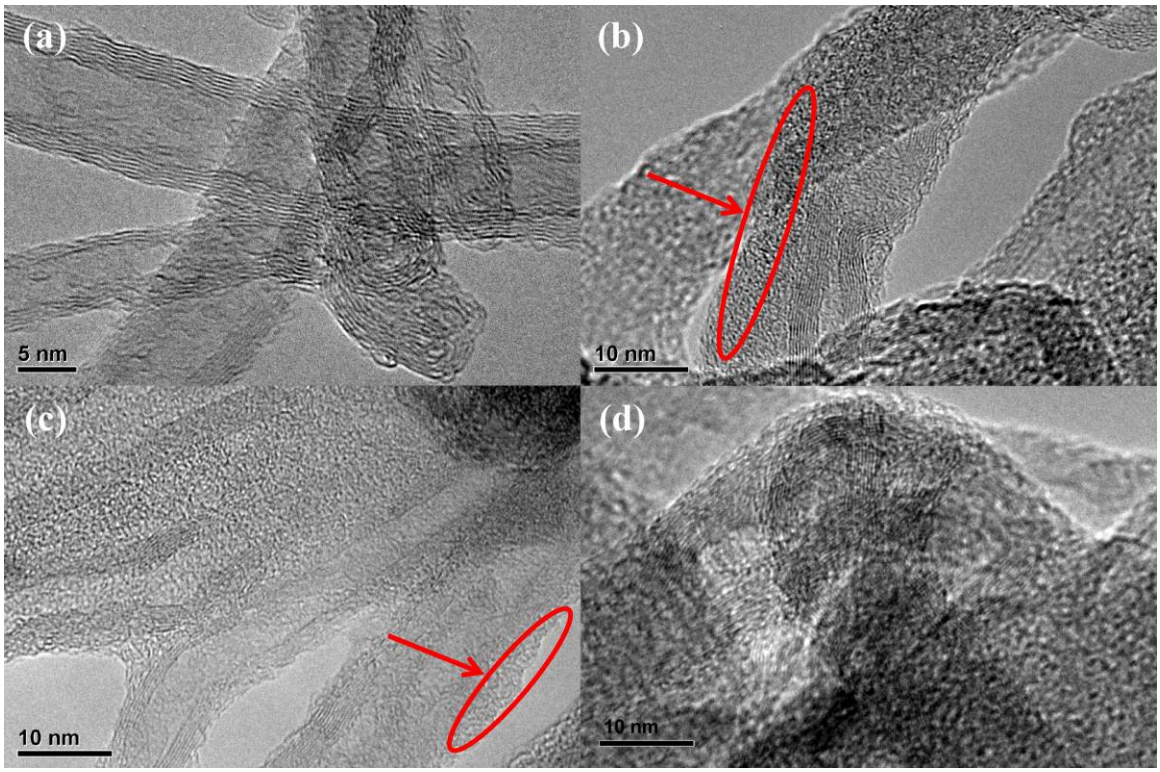

Fig. S2 TEM images of the (a) as-received MWNTs, (b) T5, (c) T20 and (d) T205.

S3. FT-IR

Fig. S3A shows the FT-IR spectra of the as-received MWNTs, pure PANI and the PNCs of T205, TA05, TCr205. The FT-IR spectra of the T5, T10, T20 samples are shown in Fig. S3B. In the FT-IR spectrum of the as-received MWNTs, Fig. S3A-a, no obvious absorption peaks are observed and are consisted with the reported few functional groups on the surface of the as-received MWNTs.[2] The absorption peaks at 1560 and 1470 cm^{-1} for pure PANI, Fig.S3A-b, correspond to the C=C stretching vibration of the quinoid and benzenoid rings in PANI, respectively.[3] The band at 1285 cm^{-1} is related to the C-N stretching vibration of the benzenoid unit in PANI. The bands at 1234 and 1114 cm^{-1} are assigned to the C-H in-plane and C-N stretching vibrations of the quinoid rings in PANI, respectively. The out-of-plane bending of the C-H in the substituted benzenoid ring of

PANI is reflected in the peak of 782 cm^{-1}.[4] These peaks are also observed in the FT-IR spectra of T205, TA05, T5, T10, T20 PNCs, however, the peak shift is clearly observed in these PNCs, indicating an interfacial interaction between the MWNTs and the hosting PANI.[5] For example, the peak at 1234 cm^{-1}, which is C-H in-plane vibration of the quinoid rings in pure PANI, shifts to a lower wavenumber of 1221 cm^{-1} in the T20 PNCs and the band at 1285 cm^{-1}, which represents the C-N stretching vibration of the benzenoid unit in pure PANI, shifts to a higher wavenumber 1289 cm^{-1} in the T20 PNCs, Fig. S3B. The characteristic peaks at 1560, 1470, 1285, 1234, 1114 and 782 cm^{-1} indicate that the synthesized PANI is half oxidized form, i.e. "emeraldine" (EB) salt form.[6] However, for the TCr205 sample, Figure S3(A)-e, the different peak around 1119 cm^{-1} is observed, exhibiting a change upon full oxidation, which corresponds to the "pernigraniline" (PB) form of PANI.[6]

S4. XPS Spectroscopy

In order to determine the Cr element valence state after the oxidation of aniline, the XPS spectroscopy is used. Generally, for the Cr2p XPS spectrum, the characteristic bindings at 577.0 ~ 578.0 and 586.0 ~ 588.0 eV correspond to Cr(III) and the characteristic peaks for the Cr(VI) are at binding energy of 580.0 ~ 580.5 and 589.0 ~ 590.0 eV.[6] Fig. S3C shows the high resolution XPS spectra of the PANI after oxidized by Cr(VI). The observed peaks of Cr2p are located at binding energy around 576.7 and 586.3 eV, which belong to the characteristic binding energy peaks of Cr(III),[7] confirming that the presented Cr in the synthesized PANI is in the Cr(III) form. The shift is from the interaction between Cr(III) and PANI matrix, in which the Cr(III) has penetrated into the interior of the PANI instead of simple physical adsorption on the surface of the PANI as

confirmed in the previous work.[6] This indicates that the Cr(VI) has been reduced to Cr(III) after oxidation of aniline to form PANI. In the high resolution XPS spectra shown in Fig. S3C, the former binding energy peak (576.7 eV) arises from the $Cr2p_{3/2}$ orbital and the latter (586.3 eV) for the $Cr2p_{1/2}$ orbital.[8]

S5. Raman Spectroscopy

In this study, Raman spectroscopy is introduced to study further the interactions between MWNTs and PANI. In the typical Raman spectrum of the MWNTs, the G-band (E_{2g} symmetry, graphite mode) appearing at around 1580 cm^{-1} is due to the sp^2 carbon networks,[9] and the characteristic defect induced D band at around 1300 cm^{-1} arises from the sp^3 carbon networks.[10] The integrated intensity ratio of I_D/I_G for the D band and G band has been used to characterize the defect quantity in the graphitic materials.[9] Fig. 1c shows the Raman spectra of the as-received MWNTs, and the T5, T205 and TA05 PNCs with 785 nm laser excitation. A depressed G band and an increased D band are observed in the T5, T205 and TA05 PNCs compared with those of the as-received MWNTs, indicating that a certain number of structural defects have been introduced to the MWNTs with the formation of oxygen species on the sidewall of MWNTs during the nanocomposite fabrication process.[9]

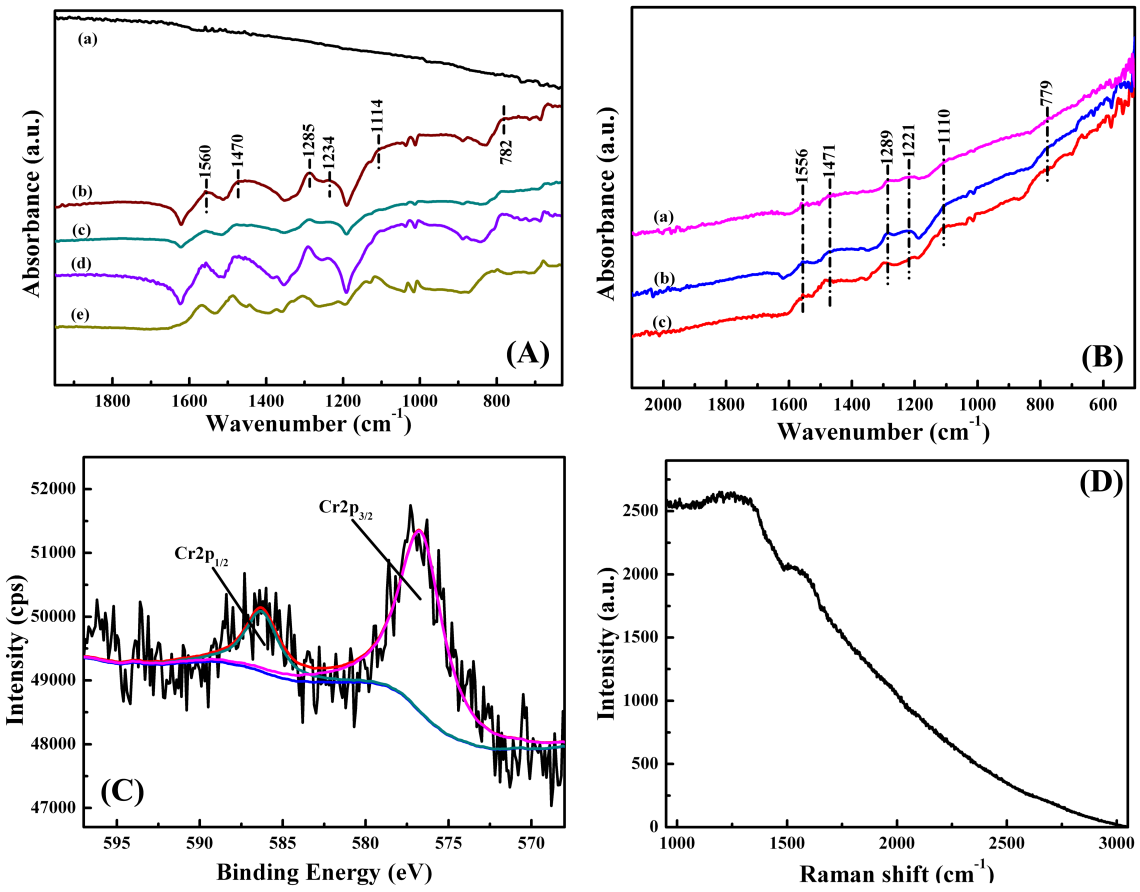

Fig. S3 (A) FT-IR spectra of (a) as-received MWNTs, (b) pure PANI oxidized by Cr(VI), (c) TA05, (d) T205, and (e) TCr205; (B) FT-IR spectra of the (a) T20, (b) T10 and (c) T5; (C) High resolution Cr2p XPS spectra of the PANI after oxidized by Cr(VI); (D) Raman spectrum of the pure PANI with 785 nm laser excitation.

S6. TGA Analysis

Fig. S4 shows the TGA results of the as-received MWNTs, pure PANI synthesized by Cr(VI) and its PNCs of TA05, T5, T10, T20, T205, TCr205. In Fig. S4(a), the MWNTs have only one-stage weight loss from 500 to 600 ^{o}C due to the thermal degradation of hexagonal carbon from the MWNTs[11] and the decomposition temperature (15% weight loss) is about 546 ^{o}C. For pure PANI synthesized by Cr(VI), only one-stage weight loss around 400 ^{o}C is observed and the decomposition temperature (15% weight loss) is about 320 ^{o}C, the significant weight loss around 120 ^{o}C in the curve is due to the loss of moisture. For the T5, T10, and T20 samples, the two-stage weight losses have

been observed. The first weight loss from 300 to 450 ^{o}C is due to the thermal degradation of the PANI chains[12] and the second weight loss from 500 to 600 ^{o}C arises from the thermal degradation of MWNTs. The different weight percentage of MWNTs (500-600 ^{o}C weight loss) in the MWNTs/PANI nanocomposites can affect the properties of nanocomposites. The 15% weight loss decomposition temperatures (5, 10, and 15 wt% loss temperature are normally used to determine the onset temperature for the decomposition. In this work, the 15 wt% is chosen to study the thermal stability of the synthesized samples.) for the T5, T10, and T20 samples (Fig. S4-a) are 375, 389 and 416 ^{o}C, respectively, which are higher than that of pure PANI (320 ^{o}C), indicating that the introduction of MWNTs in the hosting PANI matrix can increase the thermal stability of PANI, and the thermal stability increases with increasing MWNT loading. For the TCr205 sample, Fig. S4-a, there are two-stage weight loss consisting of the degradation of the PANI chains in the temperature range of 300-450 ^{o}C in the first stage and the decomposition of the MWNTs at temperatures higher than 550 ^{o}C in the second stage. The 15% weight loss temperature of TCr205 is 338 ^{o}C. For the T205 sample, Fig. S4-b, the first stage at around 250 ^{o}C is attributed to the degradation of dopant anions of PTSA,[13] the second stage (major weight loss) from 300 to 600 ^{o}C is due to a large-scale thermal degradation of the PANI chains,[6] and the 15% weight loss temperature is 337 ^{o}C. In the degradation profile of TA05 sample, Fig. S4-b, the weight loss around 120 ^{o}C is also from the loss of moisture. There are three-stage weight losses in this sample. The first stage around 250 ^{o}C is due to the degradation of dopant anions of PTSA, the second stage from 300 to 600 ^{o}C is from the large-scale thermal degradation of the PANI chains, the third stage after 600 ^{o}C is attributed to the degradation of MWNTs, and the 15%

weight loss temperature is 303 ^{o}C. The thermal stability (15% weight loss temperature) of the PNCs follows a decreasing sequence of TA05< T205< TCr205< T5, indicating that the thermal stability of the PANI synthesized by Cr(VI) is higher than that of the PANI synthesized by APS. Interestingly, the PANI synthesized by APS is observed to have a large-scale thermal degradation from 300 to 600 ^{o}C, however, the thermal degradation of the PANI synthesized by Cr(VI) has a narrower scale from 300 to 450 ^{o}C.

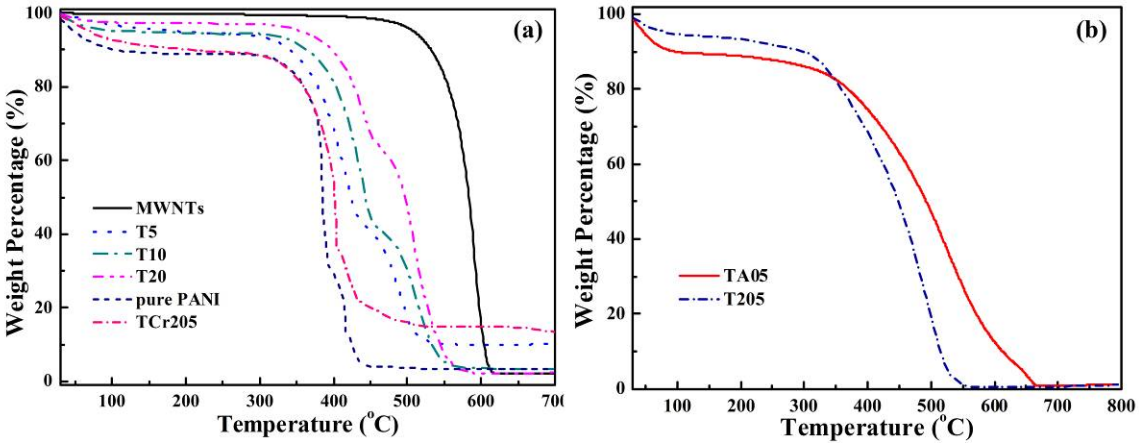

Fig. S4 TGA curves of (a) as-received MWNTs, pure PANI synthesized by Cr(VI), T5, T10, T20, TCr205; and (b) TA05, T205.

Table S1. Calculated localization length a_0 using the forward interference model for T5 sample.

Magnetic Field (T)	a_0 (μm)
0.3000	0.989
0.4000	0.981
0.5000	0.970
0.6000	0.969
0.7000	0.943
0.8000	0.901
0.9000	0.905
0.9999	0.879
1.4999	0.749
1.9999	0.679
2.4999	0.649
2.9998	0.612

Table S2 Calculated localization length a_0 using the forward interference model for T20 sample.

Magnetic Field (T)	a_0 (μm)
0.1000	
0.2000	0.778
0.3000	0.705
0.4000	0.723
0.5000	0.696
0.6000	0.740
0.7000	0.719
0.8000	0.702
0.9000	0.702
0.9999	0.700
1.4999	0.627
1.9999	0.561
2.4999	0.544
2.9998	0.524

1. H. Gu, S. B. Rapole, Y. Huang, D. Cao, Z. Luo, S. Wei and Z. Guo, *J. Mater. Chem. A*, 2013, **1**, 2011-2021.

2. H. Gu, S. Tadakamalla, X. Zhang, Y.-D. Huang, Y. Jiang, H. A. Colorado, Z. Luo, S. Wei and Z. Guo, *J. Mater. Chem. C*, 2012, **1**, 729-743.

3. J. Zhu, S. Wei, L. Zhang, Y. Mao, J. Ryu, A. B. Karki, D. P. Young and Z. Guo, *J. Mater. Chem.*, 2011, **21**, 342-348.

4. P. Mavinakuli, S. Wei, Q. Wang, A. B. Karki, S. Dhage, Z. Wang, D. P. Young and Z. Guo, *J. Phys. Chem. C*, 2010, **114**, 3874-3882.

5. H. Gu, Y. Huang, X. Zhang, Q. Wang, J. Zhu, L. Shao, N. Haldolaarachchige, D. P. Young, S. Wei and Z. Guo, *Polymer*, 2012, **53**, 801-809.

6. H. Gu, S. Rapole, J. Sharma, Y. Huang, D. Cao, H. A. Colorado, Z. Luo, N. Haldolaarachchige, D. P. Young, S. Wei and Z. Guo, *RSC Adv.*, 2012, **2**, 11007-11018.

7. D. Park, Y. S. Yun and J. M. Park, *J. Colloid Interface Sci.*, 2008, **317**, 54-61.

8. B. A. Manning, J. R. Kiser, H. Kwon and S. R. Kanel, *Environ. Sci. Technol.*, 2006, **41**, 586-592.

9. Y. C. Jung, H. H. Kim, Y. A. Kim, J. H. Kim, J. W. Cho, M. Endo and M. S. Dresselhaus, *Macromolecules*, 2010, **43**, 6106-6112.

10. D. McIntosh, V. N. Khabashesku and E. V. Barrera, *J. Phys. Chem. C*, 2007, **111**, 1592-1600.

11. A. C. Baudouin, J. Devaux and C. Bailly, *Polymer*, 2010, **51**, 1341-1354.

12. X. Feng, C. Mao, G. Yang, W. Hou and J. Zhu, *Langmuir*, 2006, **22**, 4384-4389.

13. H. Gu, S. Tadakamalla, Y. Huang, H. A. Colorado, Z. Luo, N. Haldolaarachchige, D. P. Young, S. Wei and Z. Guo, *ACS Appl. Mater. Interfaces*, 2012, **4**, 5613-5624.